Science & Technology Development Journal – Engineering and Technology 2023, 6(1):1844-1854

Open Access Full Text Article

Research Article

Dynamic behavior of sandwich beam with agglomerated carbon nanotube reinforced face sheets under a moving mass

Thom T. Tran[*], **Hoai T. T. Bui**, **Kien D. Nguyen**

ABSTRACT

In this paper, the dynamic behavior of carbon nanotube (CNT) reinforced composite sandwich beams under a moving mass taking into account the influence of the CNT agglomeration is investigated by the finite element method. The sandwich beams composed of a homogeneous core and two face layers made from carbon nanotube–reinforced composite (CNTRC) material. The two-parameter micromechanical model is adopted to describe the agglomeration of the CNTs, and the Eshelby–Mori–Tanaka approach is used to estimate the effective material properties of the composite face layers. Based on a third-order shear deformation beam theory, a beam element in which the transverse shear rotation, not the conventional section rotation, is employed as an independent variable is formulated and used to establish the discretized equation of motion for the beams. Using an implicit Newmark method, dynamic characteristics such as the time histories for mid-span deflections and the dynamic magnification factors are obtained for a sandwich beam with simply supported ends. The accuracy of the derived beam element is confirmed by comparing the results obtained in the present work with the published data. The numerical result reveals that the CNT volume fraction and the CNT agglomeration have a significant influence on the dynamic response of the sandwich beams. The dynamic magnification factor is found to be decreased with an increase of the CNT volume fraction, but it is higher for the case of the severse CNT agglomeration. A parametric study carried out to highlight the effects of the CNT reinforcement and the mass velocity on the dynamic behavior of the sandwich beams. The influence of the layer thickness ratio on the dynamic response of the composite sandwich beams is also studied and discussed.

Key words: Agglomerated CNTRC sandwich beam, moving mass, third-order theory, dynamic analysis

Institute of Mechanics, VAST, 18 Hoang Quoc Viet, Hanoi, Viet Nam

Correspondence

Thom T. Tran, Institute of Mechanics, VAST, 18 Hoang Quoc Viet, Hanoi, Viet Nam

Email: ttthom@imech.vast.vn

History

- Received: 01-12-2022
- Accepted: 23-5-2023
- Published Online: 30-6-2023

DOI :

https://doi.org/10.32508/stdjet.v6i1.1054

INTRODUCTION

Carbon nanotubes with outstanding mechanical, thermal, electrical and physical properties have wide applications in engineering. The use of CNTs in improving properties of the conventional composites has been studied by many scientists. However, in most studies the CNTs are considered as aligned single-walled carbon nanotubes, the properties of the composite are evaluated through rule of mixture model (ROM) [1–10].

CNTs tend to agglomerate due to their high aspect ratio, low bending rigidity, and this causes the fabrication of composites with uniformly distributed CNTs a serious challenge. Shi et al. [11] developed a micromechanics model considering the influence of CNT agglomeration. Thereafter, Heshmati and Yas [12] presented a numerical analysis on vibration of functionally graded CNTRC (FG-CNTRC) beam using Eshelby-Mori-Tanaka (E-M-T) approach. In there, the two parameters micromechanics model [11] was adopted to account for the influence of CNT agglomeration on elastic properties of randomly oriented CNTRC, and the Mori-Tanaka (M-T) scheme was adopted to estimate effective moduli of the composite. Different CNT distributions in the beam thickness have been considered in evaluating the frequencies of the beam in reference [12]. It is worthy to note that the finite element model in reference [12] is converged by using a very fine mesh, namely 100 elements. Nejati and Eslampanah [13] adopted the differential quadrature method (DQM) to compute frequencies of a thick FG-CNTRC beam. The effect of agglomerated CNTs on natural frequencies of the composite beam was also investigated in reference [13]. Timoshenko beam theory and the DQM were used by Kamarian et al. [14] to study free vibration of nanocomposite sandwich beams resting on Pasternak foundation, taking into account the influence of CNT agglomeration. The CNT volume fraction of the beam faces in reference [14] is graded by four parameter power-law distributions. The vibration analysis of non-uniform CNTRC beams integrated with piezoelectric layers was presented by Kamarian et al. [15], taking into account the CNT agglomeration effect. Recently, Kiani

Cite this article : Tran T T, Bui H T T, Nguyen K D. **Dynamic behavior of sandwich beam with agglomerated carbon nanotube reinforced face sheets under a moving mass**. *Sci. Tech. Dev. J. – Engineering and Technology* 2023; 6(1):1844-1854.

et al.[16] investigated thermo-mechanical buckling of CNTRC beams under a non-uniform thermal loading. Governing equations for the beams are constructed through Hamilton's principle, and they are solved by the DQM.

This paper studies dynamic behavior of agglomerated CNTRC sandwich beams under a moving mass for the first time. The sandwich beams composed of a homogeneous core and two face sheets made from CNTRC material. The E-M-T approach considering the influence of the CNTs agglomeration is adopted in estimating the effective properties of the face layers. A third-order shear deformable beam element is formulated and used to construct the equation of motion of the beams. Using Newmark method, dynamic characteristics such as the time histories for mid-span deflections and dynamic magnification factors are computed for the beam with simply supported ends. The effects of the CNT reinforcement, CNT agglomeration, mass velocity as well as the length-to-height ratio on the dynamic behavior of the sandwich beams are examined in detail.

COMPOSITE BEAM REINFORCED WITH AGGLOMERATED CNTS

A simply supported sandwich beam with length L, cross section $b \times h$ under a mass m_c, moving with constant velocity v as depicted in Figure 1 is considered. The beam formed from a homogeneous core and two face layers made of a CNT reinforced composite. The x-axis of the Cartesian coordinate in Figure 1 is chosen on the beam's mid-plane. Denoted by $h_0 = -\frac{h}{2}$, h_1, h_2, $h_3 = \frac{h}{2}$ are, respectively, the coordinates in z-direction of the lowermost surface, the interfaces between the layers and the topmost surface.

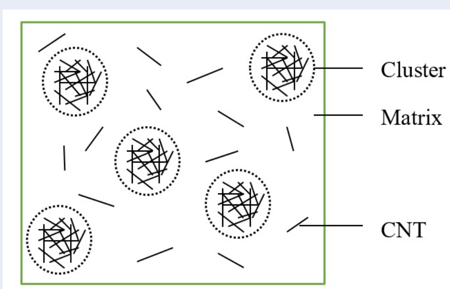

Figure 2: RVE with Eshelby cluster model of CNT agglomeration

Figure 2 shows a representative volume element (RVE) V, where there are some regions with a higher concentration CNTs, the spherical clusters. The total CNT volume V_r in the RVE can be split into the two parts as

$$V_r = V_r^{cluster} + V_r^m \tag{1}$$

in which $V_r^{cluster}$ and V_r^m represent the CNT volumes inside and outside the cluster, respectively. The CNT volume fraction V_{CNT} in the composite is $V_{CNT} = \frac{V_r}{V}$. Two parameters are used to describe the agglomeration as follows[11]

$$\xi = \frac{V_{cluster}}{V},\ \zeta = \frac{V_r^{cluster}}{V_r},\ 0 \le \xi, \zeta \le 1 \tag{2}$$

where $V_{cluster}$ is the volume of clusters in the RVE; ξ denotes the volume fraction of clusters with respect to the total volume of the RVE and ζ is the volume ratio of CNTs inside the clusters over the total CNT inside the RVE. In special case of $\xi = 1$ CNTs are uniformity distributed in the matrix, and a decrease of the parameter ξ leads to an increase of the CNT agglomeration. With $\zeta = 1$ all CNTs are inside the clusters. The case $\xi = \zeta$ means that the volume fraction of CNTs inside the clusters equals to that of CNTs outside the clusters. In the case $\zeta > \xi$, the value of ζ is bigger, the distribution of CNTs is more heterogeneous. The effective bulk and shear moduli of the clusters K_{in}, G_{in} and those of the region outside the clusters K_{out}, G_{out} may be calculated by the following form[11]

$$\begin{aligned}
K_{in} &= K_m + \frac{V_{CNT}\,\zeta\,(\delta_r - 3K_m\alpha_r)}{3\,(\xi - V_{CNT}\,\zeta + V_{CNT}\,\zeta\,\alpha_r)};\\
G_{in} &= G_m + \frac{V_{CNT}\,\zeta\,(\eta_r - 2G_m\beta_r)}{2\,(\xi - V_{CNT}\,\zeta + V_{CNT}\,\zeta\,\beta_r)};\\
K_{out} &= K_m + \frac{V_{CNT}\,(1-\zeta)\,(\delta_r - 3K_m\alpha_r)}{3\,[1-\xi - V_{CNT}\,(1-\zeta) + V_{CNT}\,(1-\zeta)\,\alpha_r]};\\
G_{out} &= G_m + \frac{V_{CNT}\,(1-\zeta)\,(\eta_r - 2G_m\beta_r)}{2\,[1-\xi - V_{CNT}\,(1-\zeta) + V_{CNT}\,(1-\zeta)\,\zeta\beta_r]}
\end{aligned} \tag{3}$$

with

$$\begin{aligned}
\alpha_r &= \frac{3(K_m+G_m)+k_r-l_r}{3(G_m+k_r)};\\
\delta_r &= \frac{1}{3}\left[n_r + 2l_r + \frac{(2k_r+l_r)(3K_m+2G_m-l_r)}{G_m+k_r}\right];\\
\beta_r &= \frac{1}{5}\left(\frac{4G_m+2k_r+l_r}{3(G_m+k_r)} + \frac{4G_m}{G_m+p_r} + \frac{2[G_m(3K_m+G_m)+G_m(3K_m+7G_m)]}{G_m(3K_m+G_m)+m_r(3K_m+7G_m)}\right);\\
\eta_r &= \frac{1}{5}\left[\frac{2}{3}(n_r - l_r) + \frac{8G_m p_r}{G_m+p_r} + \frac{8m_rG_m(3K_m+4G_m)}{3K_m(m_r+G_m)+G_m(7m_r+G_m)} + \frac{(2k_r-l_r)(2G_m+l_r)}{3(G_m+k_r)}\right];
\end{aligned} \tag{4}$$

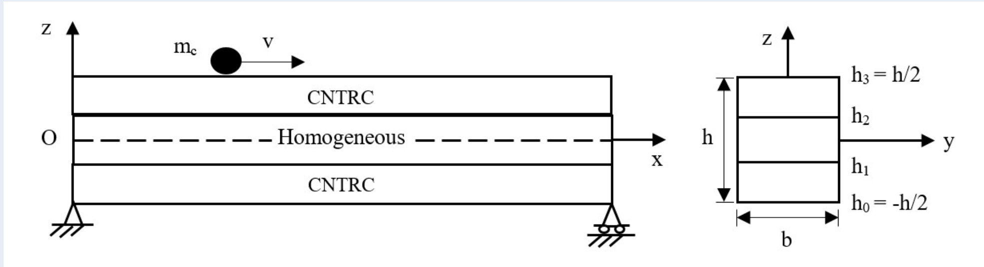

Figure 1: CNTRC sandwich beam under a moving mass

where $K_m = \frac{E_m}{3(1-2\nu_m)}$, $G_m = \frac{E_m}{2(1+\nu_m)}$ are the bulk and shear moduli of the matrix, respectively. The subscripts m and r in Eqs. (3) and (4) denote the quantities of the matrix and the reinforcing phase (CNTs); k_r, l_r, m_r, n_r, p_r are the Hill's elastic moduli for the reinforcing phase.

The effective bulk and shear moduli of the composite estimated by the M-T method are of the forms [11]

$$\begin{aligned} K &= K_{out}\left(1+\frac{\xi\left(\frac{K_{in}}{K_{out}}-1\right)}{1+\alpha\left(1-\xi\right)\left(\frac{K_{in}}{K_{out}}-1\right)}\right); \\ G &= G_{out}\left(1+\frac{\xi\left(\frac{G_{in}}{G_{out}}-1\right)}{1+\beta\left(1-\xi\right)\left(\frac{G_{in}}{G_{out}}-1\right)}\right) \end{aligned} \tag{5}$$

where

$$\begin{aligned} \alpha &= \frac{1+\nu_{out}}{3\left(1-\nu_{out}\right)};\ \beta = \frac{8-10\nu_{out}}{15\left(1-\nu_{out}\right)}; \\ \nu_{out} &= \frac{\left(3K_{out}-2G_{out}\right)}{2\left(3K_{out}+G_{out}\right)} \end{aligned} \tag{6}$$

Noting that in the case CNTs are randomly distributed throughout the matrix, the composite is considered to be isotropic. Then, the bulk and shear moduli have the following forms [11]

$$\begin{aligned} K &= K_m + \frac{V_{CNT}\left(\delta_r - 3K_m\alpha_r\right)}{3(c_m+V_{CNT}\alpha_r)}; \\ G &= G_m + \frac{V_{CNT}\left(\eta_r - 2G_m\beta_r\right)}{2(c_m+V_{CNT}\beta_r)}; \end{aligned}$$

where $c_m = 1 - V_{CNT}$, and α_r, δ_r, β_r, η_r are given by Eq. (4).

The Young's modulus E and Poisson's ratio ν of the composite layers are computed as

$$E = \frac{9KG}{3K+G};\ \nu = \frac{3K-2G}{6K+2G} \tag{8}$$

The equivalent density of the composite layers is simply calculated as follows [17]

$$\rho = \left(\rho^{CNT} - \rho^{m}\right)V_{CNT} + \rho^{m} \tag{9}$$

MATHEMATICAL FORMULATION

The axial and transverse displacements of a point in the beam based on the shear deformation theory [18] are of the form

$$\begin{aligned} u\left(x,z,t\right) &= u_0\left(x,t\right) + \frac{z}{4}\left(5\theta + w_{0,x}\right) \\ &\quad - \frac{5z^3}{3h^2}\left(\theta + w_{0,x}\right) \\ w\left(x,z,t\right) &= w_0\left(x,t\right) \end{aligned} \tag{10}$$

where $u_0\left(x,t\right)$, $w_0\left(x,t\right)$ represent the components of displacement at $z=0$; θ is the rotation of the cross-section, and t is the time. The subscript comma in (10) as well as in the below denotes the derivative with respect the followed variable.

In order to improve the efficiency of the finite element formulation in the next section, instead of the rotation θ, we adopted herein the transverse shear rotation γ_0, defined as follows [19,20] $\gamma_0 = \theta + w_{0,x}$ as an independent variable. In this regard, the displacements in Eq. (10) can be recast as

$$\begin{aligned} u\left(x,z,t\right) &= u_0\left(x,t\right) \\ &\quad + z\left(\frac{5}{4}\gamma_0 - w_{0,x}\right) - \frac{5z^3}{3h^2}\gamma_0 \\ w\left(x,z,t\right) &= w_0\left(x,t\right) \end{aligned} \tag{11}$$

The normal strain ε_{xx} and shear strain γ_{xz} resulted from Eq. (11) are as follows

$$\begin{aligned} \varepsilon_{xx} &= u_{0,x} \\ &\quad + z\left(\frac{5}{4}\gamma_{0,x} - w_{0,xx}\right) - \frac{5z^3}{3h^2}\gamma_{0,x} \\ \gamma_{xz} &= 5\left(\frac{1}{4} - \frac{1}{h^2}z^2\right)\gamma_0 \end{aligned} \tag{12}$$

The constitutive relation based on the assumption of material linear behavior is as follows

$$\sigma_{xx} = E\varepsilon_{xx};\ \tau_{xz} = G\gamma_{xz} \tag{13}$$

The strain energy for the sandwich beam U is

$$\begin{aligned}U &= \frac{1}{2}\int_V (\sigma_{xx}\varepsilon_{xx} + \tau_{xz}\gamma_{xz})\,dV \\ &= \frac{1}{2}\int_0^L [A_{11}u_{0,x}^2 + 2A_{12}u_{0,x}\left(\frac{5}{4}\gamma_{0,x} - w_{0,xx}\right) \\ &+A_{22}\left(\frac{5}{4}\gamma_{0,x} - w_{0,xx}\right)^2 - \frac{10}{3h^2}A_{34}u_{0,x}\gamma_{0,x} \\ &-\frac{10}{3h^2}A_{44}\gamma_{0,x}\left(\frac{5}{4}\gamma_{0,x} - w_{0,xx}\right) + \frac{25}{9h^4}A_{66}\gamma_{0,x}^2 \\ &+25\left(\frac{1}{16}B_{11} - \frac{1}{2h^2}B_{22} + \frac{1}{h^4}B_{44}\right)\gamma_0^2]\end{aligned} \tag{14}$$

where $A_{11}, A_{12}, \ldots, A_{66}$ and B_{11}, B_{22}, B_{44} are the beam rigidities, defined as

$$\begin{aligned}&(A_{11}, A_{12}, A_{22}, A_{34}, A_{44}, A_{66}) \\ &= b\int_{h_0}^{h_3} E\left(1, z, z^2, z^3, z^4, z^6\right)dz \\ &= b\sum_{k=1}^{3}\int_{h_{k-1}}^{h_k} E^{(k)}\left(1, z, z^2, z^3, z^4, z^6\right)dz; \\ &(B_{11}, B_{22}, B_{44}) = b\int_{h_0}^{h_3} G\left(1, z^2, z^4\right)dz \\ &= b\sum_{k=1}^{3}\int_{h_{k-1}}^{h_k} G^{(k)}\left(1, z^2, z^4\right)dz\end{aligned} \tag{15}$$

The kinetic energy T of the sandwich beam is given by

$$\begin{aligned}T &= \frac{1}{2}\int_0^L \int_A \rho\left(\dot{u}^2 + \dot{w}^2\right)dA\,dx \\ &= \frac{1}{2}\int_0^L [I_{11}\left(\dot{u}_0^2 + \dot{w}_0^2\right) + 2I_{12}\dot{u}_0\left(\frac{5}{4}\dot{\gamma}_0 - \dot{w}_{0,x}\right) \\ &+I_{22}\left(\frac{5}{4}\dot{\gamma}_0 - \dot{w}_{0,x}\right)^2 - \frac{10}{3h^2}I_{34}\dot{u}_0\dot{\gamma}_0 \\ &-\frac{10}{3h^2}I_{44}\dot{\gamma}_0\left(\frac{5}{4}\dot{\gamma}_0 - \dot{w}_{0,x}\right) + \frac{25}{9h^4}I_{66}\dot{\gamma}_0^2]dx\end{aligned} \tag{16}$$

In the above equations, the over dot denotes the derivative with respect to time; $I_{11},\ I_{12},\ \ldots,\ I_{66}$ are the mass moments, defined as

$$\begin{aligned}&(I_{11},\ I_{12},\ I_{22},\ I_{34},\ I_{44},\ I_{66}) \\ &= b\int_{h_0}^{h_3} \rho\left(1, z, z^2, z^3, z^4, z^6\right)dz \\ &= b\sum_{k=1}^{3}\int_{h_{k-1}}^{h_k} \rho^{(k)}\left(1, z, z^2, z^3, z^4, z^6\right)dz\end{aligned} \tag{17}$$

The potential energy due to the moving mass is given by

$$\begin{aligned}V = &-\int_0^L [(m_c g - m_c\ddot{w}_0 - 2m_c v\dot{w}_{0,x} \\ &-m_c v^2 w_{0,xx})w_0 - m_c\ddot{u}_0 u_0]\,\delta(x - vt)\,dx\end{aligned} \tag{18}$$

where g = 9.81 m/s^2 is the acceleration of gravity, $m_c\ddot{u}_0$ and $m_c\ddot{w}_0$ are the inertial forces; $2m_c v\dot{w}_{0,x}$ and $m_c v^2 w_{0,xx}$ are, respectively, the Coriolis and centrifugal forces; $\delta(.)$ denotes the Dirac delta function; x is the current abscissa of the mass, calculated from the left support. It is worthy to note that the transverse displacement w in Eq. (18) is evaluated at $z = 0$.

METHODOLOGY

The finite element method is used herein to compute dynamic response of the sandwich beam. To this end, a two-node beam element with length l is considered herewith. The vector of degrees of freedom for the element ($\mathbf{d}$) has eight components as

$$\mathbf{d} = \left\{\mathbf{d}_{\mathrm{u}} \quad \mathbf{d}_{\mathrm{w}} \quad \mathbf{d}_{\gamma}\right\}^T \tag{19}$$

where

$$\begin{aligned}&\mathbf{d}_{\mathrm{u}} = \left\{u_{01} \quad u_{02}\right\}^T;\ \mathbf{d}_{\gamma} = \left\{\gamma_{01} \quad \gamma_{02}\right\}^T \\ &\mathbf{d}_{\mathrm{w}} = \left\{w_{01} \quad w_{0x1} \quad w_{02} \quad w_{0x2}\right\}^T;\end{aligned} \tag{20}$$

are, respectively, the vectors of nodal displacement for u_0, w_0 and γ_0 at nodes 1 and 2. The superscript 'T' in the above equations and in the below indicates the transpose of a vector or a matrix. The axial displacement u_0 and transverse shear rotation γ_0 are linealy interpolated from its nodal values, while the transverse displacement w_0 is interpolated by using Hermite polynomials as

$$u_0 = \mathbf{N}\mathbf{d}_{\mathrm{u}};\ w_0 = \mathbf{H}\mathbf{d}_{\mathrm{w}};\ \gamma_0 = \mathbf{N}\mathbf{d}_{\gamma} \tag{21}$$

where $\mathbf{N} = \left\{N_1 \quad N_2\right\}, \mathbf{H} = \left\{H_1 \quad H_2 \quad H_3 \quad H_4\right\}$ in which

$$N_1 = 1 - \frac{x}{l},\ N_2 = \frac{x}{l} \tag{22}$$

and

$$\begin{aligned}&H_1 = 1 - 3\left(\frac{x}{l}\right)^2 + 2\left(\frac{x}{l}\right)^3; \\ &H_2 = x - 2\frac{x^2}{l} + \frac{x^3}{l^2}; \\ &H_3 = 3\left(\frac{x}{l}\right)^2 - 2\left(\frac{x}{l}\right)^3; \\ &H_4 = -\frac{x^2}{l} + \frac{x^3}{l^2}\end{aligned} \tag{23}$$

With the interpolations, one can write the strain energy in Eq. (14) in the form

$$U = \frac{1}{2}\sum^{ne}\mathbf{d}^{\mathbf{T}}\mathbf{k}\mathbf{d} \tag{24}$$

where ne is the number of elements, and the element stiffness matrix $\boldsymbol{k}$ can be split into sub-matrices as

$$\mathbf{k} = \begin{bmatrix}\mathbf{k}_{uu} & \mathbf{k}_{uw} & \mathbf{k}_{u\gamma} \\ \mathbf{k}_{uw}^T & \mathbf{k}_{ww} & \mathbf{k}_{w\gamma} \\ \mathbf{k}_{u\gamma}^T & \mathbf{k}_{w\gamma}^T & \mathbf{k}_{\gamma\gamma}\end{bmatrix} \tag{25}$$

In the above equation, $\mathbf{k}_{uu},\ \mathbf{k}_{uw},\ \ldots,\ \mathbf{k}_{\gamma\gamma}$ are, respectively, the element stiffness matrices resulted from the axial stretching, bending, shear deformation and their couplings. The expressions of these sub-matrices are as follows

$$\begin{aligned}
&\mathbf{k}_{uu}=\int_0^l \mathbf{N}_{,x}^T A_{11}\mathbf{N}_{,x}dx;\ \mathbf{k}_{uw}=\int_0^l \mathbf{N}_{,x}^T \mathrm{A}_{12}\mathbf{H}_{,xx}dx;\\
&\mathbf{k}_{u\gamma}=5\int_0^l\left(\tfrac{1}{4}\mathbf{N}_{,x}^T\mathrm{A}_{12}\mathbf{N}_{,x}-\tfrac{1}{3h^2}\int_0^l\mathbf{N}_{,x}^T\mathrm{A}_{34}\mathbf{N}_{,x}\right)dx;\\
&\mathbf{k}_{ww}=\int_0^l\mathbf{H}_{,xx}^T\mathrm{A}_{22}\mathbf{H}_{,xx}dx;\\
&\mathbf{k}_{w\gamma}=5\int_0^l\left(-\tfrac{1}{4}\mathbf{H}_{,xx}^T\mathrm{A}_{22}\mathbf{N}_{,x}+\tfrac{1}{3h^2}\int_0^l\mathbf{H}_{,xx}^T\mathrm{A}_{44}\mathbf{N}_{,x}\right)dx;\\
&\mathbf{k}_{\gamma\gamma}=25\int_0^l[\tfrac{1}{16}\mathbf{N}_{,x}^T\mathrm{A}_{22}\mathbf{N}_{,x}-\tfrac{1}{12h^2}\mathbf{N}_{,x}^T\mathrm{A}_{44}\mathbf{N}_{,x}\\
&+\tfrac{1}{9h^4}\mathbf{N}_{,x}^T\mathrm{A}_{66}\mathbf{N}_{,x}\\
&+\mathbf{N}^T\left(\tfrac{1}{16}\mathrm{B}_{11}-\tfrac{1}{2h^2}\mathrm{B}_{22}+\tfrac{1}{h^4}\mathrm{B}_{44}\right)\mathbf{N}]dx
\end{aligned}\tag{26}$$

In a similar way, one can write the kinetic energy in Eq. (16) in the form

$$T=\frac{1}{2}\sum^{ne}\dot{\mathbf{d}}^{\mathbf{T}}\mathbf{m}\dot{\mathbf{d}}\tag{27}$$

where $\boldsymbol{m}$ is the element mass matrix, which can also split as

$$\mathbf{m}=\begin{bmatrix}\mathbf{m}_{uu} & \mathbf{m}_{uw} & \mathbf{m}_{u\gamma}\\ \mathbf{m}_{uw}^T & \mathbf{m}_{ww} & \mathbf{m}_{w\gamma}\\ \mathbf{m}_{u\gamma}^T & \mathbf{m}_{w\gamma}^T & \mathbf{m}_{\gamma\gamma}\end{bmatrix}\tag{28}$$

The detail expressions of the sub-matrices in Eq. (28) are

$$\begin{aligned}
&\mathbf{m}_{\mathrm{uu}}=\int_0^{\mathrm{l}}\mathbf{N}^{\mathrm{T}}\mathrm{I}_{11}\mathbf{N}\mathrm{dx};\ \mathbf{m}_{\mathrm{uw}}=-\int_0^{\mathrm{l}}\mathbf{N}^{\mathrm{T}}\mathrm{I}_{12}\mathbf{H}_{,\mathrm{x}}\mathrm{dx}\\
&\mathbf{m}_{\mathrm{u}\gamma}=5\left(\tfrac{1}{4}\mathbf{N}^{\mathrm{T}}\mathrm{I}_{12}\mathbf{N}-\tfrac{1}{3\mathrm{h}^2}\mathbf{N}^{\mathrm{T}}\mathrm{I}_{34}\mathbf{N}\right)\mathrm{dx};\\
&\mathbf{m}_{\mathrm{ww}}=\int_0^{\mathrm{l}}\left(\mathbf{H}^{\mathrm{T}}\mathrm{I}_{11}\mathbf{H}+\mathbf{H}_{,\mathrm{x}}^{\mathrm{T}}\mathrm{I}_{22}\mathbf{H}_{,\mathrm{x}}\right)\mathrm{dx};\\
&\mathbf{m}_{\gamma\gamma}=25\int_0^{\mathrm{l}}\mathbf{N}^{\mathrm{T}}\left(\tfrac{1}{16}\mathrm{I}_{22}-\tfrac{1}{2\mathrm{h}^2}\mathrm{I}_{44}+\tfrac{1}{\mathrm{h}^4}\mathrm{I}_{66}\right)\mathbf{N}\mathrm{dx}
\end{aligned}\tag{29}$$

The potential energy in (18) can also written in the form

$$\begin{aligned}
&\mathrm{V}=\sum^{\mathrm{ne}}(\ddot{\mathbf{d}}^{\mathrm{T}}\mathbf{m}_{\mathrm{m}}\ddot{\mathbf{d}}+\\
&\dot{\mathbf{d}}^{\mathrm{T}}\mathbf{c}_{\mathrm{m}}\dot{\mathbf{d}}+\mathbf{d}^{\mathrm{T}}\mathbf{k}_{\mathrm{m}}\mathbf{d}-\mathbf{d}^{\mathrm{T}}\mathbf{f}_{\mathrm{m}}),
\end{aligned}\tag{30}$$

where $\mathbf{m_m}$, $\mathbf{c_m}$ and $\mathbf{k}_{\mathrm{m}}$ are the mass, damping and stiffness matrices resulted from the effect of the inertia, Coriolis and the centrifugal forces of the moving mass, respectively; $\mathbf{f}_{\mathrm{m}}$ is the time dependent nodal load vector generated by the moving mass. These matrices and vector have the following forms

$$\begin{aligned}
&\underset{10\mathrm{x}10}{\mathbf{m}_{\mathrm{m}}}=\mathrm{m_c}\begin{bmatrix}\mathbf{N^TN} & \mathbf{0} & \mathbf{0}\\ \mathbf{0} & \mathbf{H^TH} & \mathbf{0}\\ \mathbf{0} & \mathbf{0} & \mathbf{0}\end{bmatrix}_{\mathrm{x_e}};\\
&\underset{10\mathrm{x}10}{\mathbf{c}_{\mathrm{m}}}=2\mathrm{m_c}v\begin{bmatrix}\mathbf{0} & \mathbf{0} & \mathbf{0}\\ \mathbf{0} & \mathbf{H^TH_{,x}} & \mathbf{0}\\ \mathbf{0} & \mathbf{0} & \mathbf{0}\end{bmatrix}_{\mathrm{x_e}};\\
&\underset{10\mathrm{x}10}{\mathbf{k}_{\mathrm{m}}}=\mathrm{m_c}v^2\begin{bmatrix}\mathbf{0} & \mathbf{0} & \mathbf{0}\\ \mathbf{0} & \mathbf{H^TH_{,xx}} & \mathbf{0}\\ \mathbf{0} & \mathbf{0} & \mathbf{0}\end{bmatrix}_{\mathrm{x_e}};\\
&\underset{10\mathrm{x}10}{\mathbf{f}_{\mathrm{m}}}=\mathrm{m_c g}\left\{\mathbf{N^T}\quad\mathbf{H^T}\quad\mathbf{0}\right\}_{\mathrm{x_e}}^{\mathrm{T}}
\end{aligned}\tag{31}$$

where $(.)|_{x_e}$ denotes the expression (.) being evaluated at x_e- the current abscissa of the mass measured from the element left node. Thus, the matrices $\mathbf{m}_{\mathrm{m}}$, $\mathbf{c}_{\mathrm{m}}$, $\mathbf{k}_{\mathrm{m}}$ and the vector $\mathbf{f}_{\mathrm{m}}$ are zeros for all elements, except for the element under the mass.

Using the derived element stiffness and mass matrices, one can establish the equation of motion for the sandwich beam in the form

$$\mathbf{M}(t)\ddot{\mathbf{D}}+\mathbf{C}(t)\dot{\mathbf{D}}+\mathbf{K}(t)\mathbf{D}=\mathbf{F}^{ex}(t)\tag{32}$$

where **M**, **C**, **K** are the global mass, damping and stiffness matrices, respectively. These matrices have two parts, one is from the sandwich beam and the other is the time-dependent ones due to the effects of interaction forces of the moving mass with beam. The Rayleigh damping type with a damping ratio of 0.5% is adopted herein for the global damping matrix. The average acceleration Newmark method [21] is employed in the present work to solve Eq. (32).

NUMERICAL RESULTS AND DISCUSSION

Dynamic behavior of the simply supported composie sandwich beam with agglomerated CNTs under the moving mass is numerically investigated in this section. The material properties of the matrix are $E_m = 10GPa,\ \rho_m = 1150kg/m^3,\ \nu_m = 0.3$. The armchair (10,10) SWCNTs are used as the reinforcements with $\rho^{CNT} = 1400\ kg/m^3$ and representative elastic constants for SWCNTs are tabulated in Table 1. The material in matrix phase is selected as material for the core. A sandwich beam with $L/h = 20,\ b = 0.4m,\ h = 1m$ is considered herewith. Three numbers in parentheses, e.g. (2-1-1), are employed in the below to indicate the ratio of the layer thickness, from the bottom to the topmost layer.

A moving mass $m_c = 0.5\rho_m AL$ is assumed. To facilitate the discussion, we introduce the dynamic magnification factor (DMF) D_d as follows

$$D_d = max\left(\frac{w(L/2,t)}{w_{st}}\right),\tag{33}$$

where $w_{st} = m_c g L^3/48E^c I$ is the deflection of a beam made from pure core material under static load $m_c g$ at mid-span; I is the inertia moment of area of the cross-section. A time step $\triangle t = \triangle T/200$ with $\triangle T$ is the total time necessary for the mass crossing the beam, is adopted for the Newmark method.

Table 1: Hill's elastic modulus for the CNTs [11]

CNT radius $(\mathring{A})$	k_r (GPa)	l_r (GPa)	m_r (GPa)	n_r (GPa)	p_r (GPa)
10	30	10	1	450	1

Formulation verification

In order to examine the accuracy and reliability of the present study, the effective Young's modulus of an agglomerated randomly oriented CNTRC beam obtained herein are compared with that of Daghigh et al. [11] in Figure 3. The effect of agglomeration parameters ζ and ξ on the effective Young's modulus is displayed in the figure. The Young's modulus for material in matrix phase is $E_m = 2.5\ GPa$; Hill's elastic modulus for the CNTs are given in Table 1. The elastic modulus curves in Figure 3 are plotted with the volume fraction of CNTs $V_{CNT} = 0.1$.

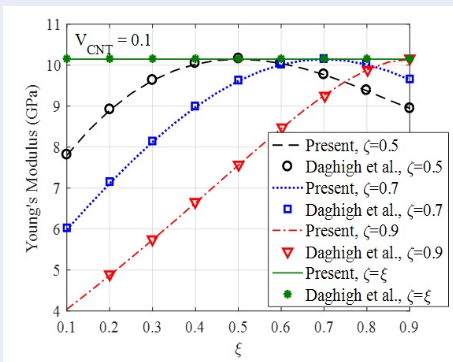

Figure 3: Comparison of CNTRC Young's modulus with $V_{CNT} = 0.1$ and different agglomeration parameters.

As can be seen from Figure 3 that Young's modulus of the present work agrees well with that of Daghigh et al. [11]. Figure 3 also shows that the agglomeration parameters have a significant effect on the Young's modulus. Specifically, the effective Young's modulus increases with the increase of ξ, its approach the highest magnitude at $\zeta = \xi$ (fully dispersed), and then Young's modulus decreases.

In Table 2, the fundamental frequency parameters of a randomly oriented CNTRC beam are compared with those of Yas and Heshmati [21]. The volume fraction of CNTs is given $V_{CNT} = 0.075$, and the frequency parameter defined as in reference [21] is $\lambda^2 = \omega L^2 \sqrt{\frac{\rho_m A}{E_m I}}$. It can be seen from the table that there is a difference in the frequency parameters obtained herein with that of Yas and Hesmati [21], but this difference is acceptable. Noting that the frequency parameters of the beam in the work by Yas and Heshmati [21] have been obtained by using 100 Timoshenko beam elements. It should be mentioned that the frequency parameters in Table 2 have been converged with a mesh of 20 elements, and this number of elements is used in all computations below.

Parametric study

In Table 3 the DMFs of the sandwich beam are given for different values of the agglomeration parameter ξ, the CNTs volume fraction V_{CNT} and layer thickness ratio. The results in Table 3 are calculated with moving mass velocity v = 100m/s, and the agglomeration parameter $\zeta = 1$. The effect of the layer thickness ratio on the DMF can be seen clearly from Table 3. As the core layer thickness increases, so the DMF of the sandwich beam increases also. This is expected since the core is not reinforced by CNTs, and an increase of the core layer leads to a decrease of sandwich beam stiffness. Besides, the agglomeration significantly affects the dependence of the DMF upon the layer thickness ratio. For example, with $V_{CNT} = 0.1$,Table 3 shows that an increase in DMF of the (1-0-1) sandwich beam compared to the (1-4-1) beam is 4.36% for a agglomeration parameter $\xi = 0.1$, while the corresponding value is 15.12% for $\xi = 1$.

As pointed out above, the decrease in parameter ξ leads to an increase in the agglomeration of CNTs. Therefore, the increase of the reinforced layer thickness might not improve significantly the dynamic response of the sandwich beam if the agglomeration is severe. Table 3 also shows the effect of the CNT volume fraction on the DMF of sandwich beam. An increase in V_{CNT} results in a marked decrease in the DMF. This phenomenon is seen more clearly when no agglomeration occurs in the sandwich beam ($\zeta = \xi = 1$). In addition, Table 3 also shows the influence of the agglomeration parameter ζ on the DMF, namely the DMF is decreased when the agglomeration parameter increases. The larger the value of V_{CNT} is, the more pronounced this effect is.

Figure 4 shows the variation of the DMF with the moving mass velocity of (1-2-1) sandwich beam for $\zeta = 1,\ \xi = 0.2$ and different the CNT volume fraction. As in case of the moving load on a FGM beam [22], the DMF in Figure 4 undergoes a repeated increase and decrease period when increasing the mass velocity v before attaining a maximum value. As expected,

Table 2: Comparison of frequency parameters of the beam reinforced with randomly oriented CNTs for different boundary conditions.

Boundary conditions	Present	Yas and Heshmati22	Error (%)
CC	5.1503	5.098585	1%
CS	4.2903	4.356794	1.55%
CF	2.0569	2.151246	4.58%
SS	3.4423	3.574603	3.84%

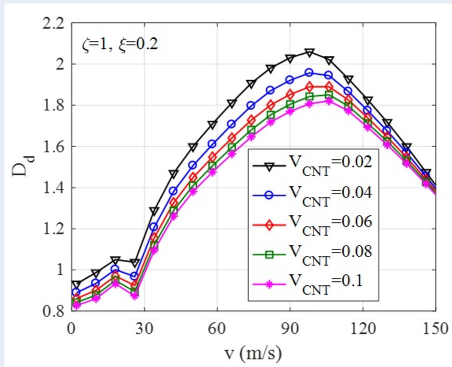

Figure 4: Variation of DMF with moving mass velocity of (1-2-1) sandwich beam for $\zeta = 1,\ \xi = 0.2$ and different the CNT volume fraction

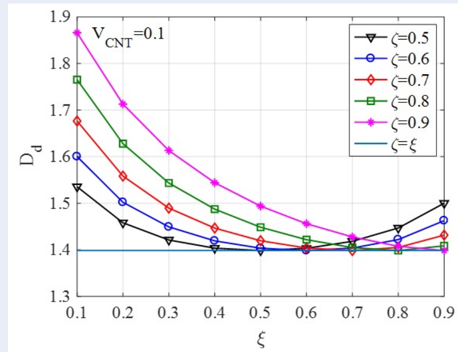

Figure 5: Relation between DMF of (1-2-1) sandwich beam with agglomeration parameters for $V_{CNT} = 0.1$,v = 100m/s

from Figure 4, the DMF is smaller when the beam associated with a higher CNT volume fraction. The moving mass velocity at which the DMF attains the maximum value is dependent on the volume fraction of CNTs.

Figure 5 shows the influence of the two agglomeration parameters on the DMF of the (1-2-1) sandwich beam for $V_{CNT} = 0.1$, and v = 100m/s. One can observe from Figure 5 that when $\xi < \zeta$, the DMF decreases by an increase of the parameter ξ, and the factor has the lowest value when $\xi = \zeta$, which correspond to the case of uniform distribution of CNTs. For $\xi > \zeta$ the DMF increases with the increase of ξ, which is opposite the case $\xi < \zeta$. From Figure 5 we can also observe that the highest DMF is achieved when the difference between the two agglomeration parameters if largest. This means that the DMF is underestimated by ignoring the aggregation of CNTs.

In order understand the dynamic behavior of FG-CNTRC sandwich beams in some deeper, we need to consider the time histories for mid-span deflection of the sandwich beams subjected by the moving mass. To this end, Figure 6 shows the time histories for deflection of (1-2-1) sandwich beam with $V_{CNT} = 0.1$,v = 50 m/s and various agglomeration parameters. It is easy to see from Figure 6 that the received mid-span deflection is the smallest at $\xi = \zeta$ ($\xi = \zeta = 1$ in Figure 6a and $\xi = \zeta = 0.2$ in Figure 6b), and it is the highest when the two agglomeration parameters are largest difference. It can be seen that the change of the agglomeration parameters only alters the magnitude of the deflection, it hardly changes the shape of the deflection curve.

CONCLUSION

The dynamics of composite sandwich beams subjected to a moving mass has been investigated in this paper in the framework of a third-order shear deformation theory. The beam composed of a homogeneous core and two face sheets of CNTRC material. The Mori-Tanaka approach, taking into consideration of CNT agglomeration is employed to derive the material properties of the CNTRC layers. A finite element formulation in which the transverse shear rotation is considered as an independent variable has been derived and used to establish the discrete equation of motion. The accuracy of the formulation has been verified by comparing the obtained result with the published work. The following main conclusions can be drawn from the present study:

Table 3: Dynamic magnification factors for sandwich beam with v = 100 m/s

	$\zeta = 1$	$V_{CNT} = 0.01$	$V_{CNT} = 0.02$	$V_{CNT} = 0.05$	$V_{CNT} = 0.1$	$V_{CNT} = 0.2$	$V_{CNT} = 0.3$
(1-0-1)	$\xi = 0.1$	2.1282	2.0740	1.9927	1.9396	1.8991	1.8793
	$\xi = 0.5$	2.1031	1.9975	1.7449	1.4874	1.2356	1.1115
	$\xi = 1$	2.0989	1.9819	1.6728	1.3185	0.9176	0.7041
(2-1-2)	$\xi = 0.1$	2.1293	2.0758	1.9957	1.9438	1.9049	1.8865
	$\xi = 0.5$	2.1044	2.0001	1.7495	1.4931	1.2421	1.1180
	$\xi = 1$	2.1003	1.9846	1.6777	1.3245	0.9238	0.7091
(1-1-1)	$\xi = 0.1$	2.1321	2.0804	2.0029	1.9527	1.9155	1.8983
	$\xi = 0.5$	2.1080	2.0068	1.7625	1.5098	1.2610	1.1373
	$\xi = 1$	2.1040	1.9917	1.6918	1.3426	0.9430	0.7262
(2-2-1)	$\xi = 0.1$	2.1382	2.0901	2.0181	1.9714	1.9366	1.9205
	$\xi = 0.5$	2.1157	2.0218	1.7931	1.5513	1.3102	1.1891
	$\xi = 1$	2.1120	2.0078	1.7260	1.3897	0.9972	0.7778
(1-2-1)	$\xi = 0.1$	2.1402	2.0933	2.0229	1.9774	1.9438	1.9285
	$\xi = 0.5$	2.1183	2.0263	1.8010	1.5604	1.3189	1.1971
	$\xi = 1$	2.1146	2.0125	1.7343	1.3984	1.0034	0.7816
(1-4-1)	$\xi = 0.1$	2.1556	2.1179	2.0612	2.0243	1.9971	1.9847
	$\xi = 0.5$	2.1380	2.0638	1.8779	1.6667	1.4436	1.3281
	$\xi = 1$	2.1350	2.0527	1.8212	1.5179	1.1389	0.9121

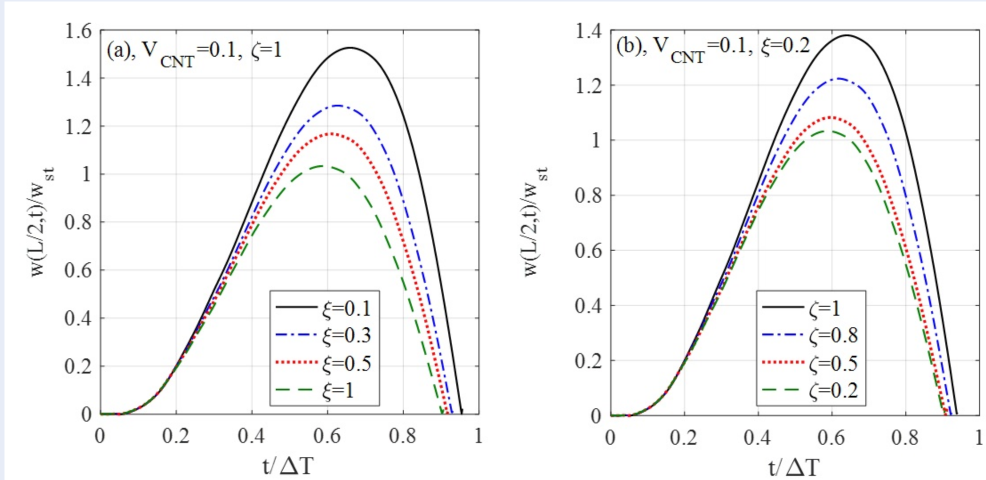

Figure 6: Time histories for mid-span deflection of (1-2-1) sandwich beam for different agglomeration parameters

1. The CNT reinforcement has a significant influence on dynamic response of the composite sandwich beams. An increase in the CNTs volume fraction leads to a sharp decrease in the DMF, especially for the case of no CNT agglomeration (fully dispersed).
2. The thickness ratio of the beam layer has a pronounced effect on the DMF of the sandwich beam. An increase of the CNT-reinforced surface layer thickness results in a significant decrease in the DMF, but this decrease is highly dependent on the volume fraction of CNTs and the agglomeration as well.
3. CNT agglomeration plays an important role in dynamic behavior of the sandwich beam. Dynamic behavior is better achieved when the two parameters agglomerate are closed to each other.

ACKNOWLEDGEMENTS

This research was made possible by the grant number CSCL03.02/22-23, Institute of Mechanics, VAST (Vietnam).

CONFLICT OF INTEREST

There is no conflict of interest.

CONTRIBUTION OF EACH AUTHOR

Thom T. Tran: validation, formal analysis, writing draft.
Hoai T. T. Bui: software.
Kien D. Nguyen: review and editing.

REFERENCES

1. Ke LL, Yang J, Kitipornchai S. Nonlinear free vibration of functionally graded carbon nanotube reinforced composite beams. Compos Struct. 2010; 92: 676-683;Available from: https://doi.org/10.1016/j.compstruct.2009.09.024.
2. Ke LL, Yang J, Kitipornchai S. Dynamic stability of functionally graded carbon nanotube reinforced composite beams. Mech Adv Mater Struct. 2013; 20: 28-37;Available from: https://doi.org/10.1080/15376494.2011.581412.
3. Yas MH, Samadi N. Free vibrations and buckling analysis of carbon nanotube reinforced composite Timoshenko beams on elastic foundation. Int J Pressure Vessels Pip. 2012; 98: 119-128;Available from: https://doi.org/10.1016/j.ijpvp.2012.07.012.
4. Shen HS, Xiang Y. Nonlinear analysis of nanotube-reinforced composite beams resting on elastic foundations in thermal environments. Eng Struct. 2013; 56: 698-708;Available from: https://doi.org/10.1016/j.engstruct.2013.06.002.
5. Ansari R, Faghih Shojaei M, Mohammadi V, Gholami R, Sadeghi F. Nonlinear forced vibration analysis of functionally graded carbon nanotube-reinforced composite Timoshenko beams. Compos Struct. 2014; 13: 316-327;Available from: https://doi.org/10.1016/j.compstruct.2014.03.015.
6. Lin F, Xiang Y. Vibration of carbon nanotube reinforced composite beams based on the first and third order beam theories. Appl Math Model. 2014; 38: 3741-3754;Available from: https://doi.org/10.1016/j.apm.2014.02.008.
7. Wu H, Kitipornchai S. Free vibration and buckling analysis of sandwich beams with functionally graded carbon nanotube-reinforced composite face sheets. Int J Struct Stab Dyn. 2015; 15(7): 1540011;Available from: https://doi.org/10.1142/S0219455415400118.
8. Wu HL, Yang J, Kitipornchai S. Nonlinear vibration of functionally graded carbon nanotube-reinforced composite beams with geometric imperfections. Compos Part B: Eng. 2016; 90: 86-96;Available from: https://doi.org/10.1016/j.compositesb.2015.12.007.
9. Ebrahimi F, Farazmandnia N. Thermo-mechanical vibration analysis of sandwich beams with functionally graded carbon nanotube-reinforced composite face sheets based on a higher-order shear deformation beam theory. Mech Adv Mater Struct. 2017; 24. https://doi.org/10.1080/15376494.2016.1196786;Available from: https://doi.org/10.1080/15376494.2016.1196786.

10. Mohseni A, Shakouri M. Vibration and stability analysis of functionally graded CNT-reinforced composite beams with variable thickness on elastic foundation. Proc IMechE Part L: J Materials: Design and Applications. 2019; 233(2): 1-12;Available from: https://doi.org/10.1177/1464420719866222.
11. Shi DL, Feng XQ, Huang YY, Hwang KC, Gao H. The effect of nanotube waviness and agglomeration on the elastic property of carbon nanotube reinforced composites. J Eng Mater Technol. 2004; 126: 250-257;Available from: https://doi.org/10.1115/1.1751182.
12. Heshmati M, Yas MH. Free vibration analysis of functionally graded CNTreinforced nanocomposite beam using Eshelby-Mori-Tanaka approach. J Mech Sci and Tech. 2013; 27(11): 3403-3408;Available from: https://doi.org/10.1007/s12206-013-0862-8.
13. Nejati M, Eslampanah A. Buckling and Vibration Analysis of Functionally Graded Carbon Nanotube-Reinforced Beam Under Axial Load. Int J Appl Mech. 2016; 8(1): 1650008;Available from: https://doi.org/10.1142/S1758825116500083.
14. Kamarian S, Shakeri M, Yas MH. Bodaghi M. and Pourasghar A. - Free vibration analysis of functionally graded nanocomposite sandwich beams resting on Pasternak foundation by considering the agglomeration effect of CNTs. J Sandwich Struct Mater. 2015; 17(6);Available from: https://doi.org/10.1177/1099636215590280.
15. Kamarian S, Bodaghi M, Pourasghar A, Talebi S. Vibrational Behavior of NonUniform Piezoelectric Sandwich Beams Made of CNT-Reinforced Polymer Nanocomposite by Considering the Agglomeration Effect of CNTs. Polym Compos 2017; 38(S1): E553-E562;Available from: https://doi.org/10.1002/pc.23933.
16. Kiani F, Ariaseresht Y, Niroumand A, Afshari H. Thermo-mechanical buckling analysis of thick beams reinforced with agglomerated CNTs with temperature-dependent thermo-mechanical properties under a nonuniform thermal loading. Mech Based Des Struct Mach. 2022;Available from: https://doi.org/10.1080/15397734.2022.2117194.
17. Daghigh H, Daghigh V. Free Vibration of Size and Temperature-Dependent Carbon Nanotube (CNT)-Reinforced Composite Nanoplates With CNT Agglomeration. Polym. Compos. 2019; 40(S2): E1479-E1494 ;Available from: https://doi.org/10.1002/pc.25057.
18. Shi G. A new simple third-order shear deformation theory of plates. Int J Solids Struct. 2007; 44: 4399-4417;Available from: https://doi.org/10.1016/j.ijsolstr.2006.11.031.
19. Shi G, Lam KY. Finite element vibration analysis of composite beams based on higher-order beam theory. J Sound Vib. 1999; 219: 707-721;Available from: https://doi.org/10.1006/jsvi.1998.1903.
20. Shi G, Lam KY, Tay TE. On efficient finite element modeling of composite beams and plates using higher-order theories and an accurate composite beam element. Compos Struct. 1998; 41: 159-165;Available from: https://doi.org/10.1016/S0263-8223(98)00050-6.
21. Yas MH, Heshmati M. Dynamic analysis of functionally graded nanocomposite beams reinforced by randomly oriented carbon nanotube under the action of moving load. Appl Math Model. 2012; 36: 1371-1394;Available from: https://doi.org/10.1016/j.apm.2011.08.037.
22. Geradin M, Rixen D. Mechanical vibrations, theory and application to structural dynamics. 2nd ed. Chichester, John Wiley & Sons (1997);.

Tạp chí Phát triển Khoa học và Công nghệ – Engineering and Technology 2023, 6(1):1844-1854

Open Access Full Text Article

Bài nghiên cứu

Ứng xử động lực học của dầm sandwich với các lớp ngoài gia cường bởi ống nano các-bon kết tụ chịu khối lượng di động sử dụng lý thuyết biến dạng trượt bậc ba

Trần Thị Thơm*, Bùi Thị Thu Hoài, Nguyễn Đình Kiên

TÓM TẮT

Trong bài báo này, ứng xử động lực học của dầm sandwich composite được gia cường các ống nano các-bon (CNT) chịu khối lượng di động trong đó có kể đến ảnh hưởng của sự kết tụ CNT được nghiên cứu bằng phương pháp phần tử hữu hạn. Dầm sandwich được tạo bởi lớp lõi thuần nhất và hai lớp ngoài được làm từ vật liệu composite gia cường các ống nano các-bon (CNTRC). Mô hình cơ học vi mô hai tham số được chấp nhận để mô tả cho sự kết tụ của CNT, và cách tiếp cận Eshelby–Mori–Tanaka được sử dụng để tối ưu các tính chất vật liệu hiệu dụng của các lớp ngoài. Dựa trên lý thuyết biến dạng trượt bậc ba, một phần tử dầm trong đó góc trượt ngang, không phải góc quay của thiết diện ngang truyền thống, được áp dụng như một biến độc lập để xây dựng và sử dụng để thiết lập các phương trình chuyển động rời rạc cho dầm. Sử dụng phương pháp tích phân trực tiếp Newmark ẩn, các đặc trưng dao động như lịch sử thời gian cho độ lệch chuẩn hóa tại giữa dầm và hệ số động lực học thu được cho dầm sandwich hai đầu tựa đơn. Tính chính xác của phần tử dầm đã được suy ra được xác nhận bằng cách so sánh các kết quả thu được trong bài báo với các kết quả đã được công bố. Kết quả số chỉ ra rằng tỉ phần thể tích CNT và sự kết tụ CNT có ảnh hưởng đáng kể lên đáp ứng động lực học của dầm sandwich. Hệ số động lực học của dầm được chỉ ra là giảm với sự tăng của tỉ phần thể tích CNT, nhưng nó lại cao hơn cho trường hợp sự kết tụ CNT là nghiêm trọng. Các nghiên cứu số cũng chỉ ra rõ nét ảnh hưởng của sự gia cường CNT và vận tốc khối lượng di động lên ứng xử động lực học của dầm sandwich. Ảnh hưởng của tỉ số chiều dày các lớp lên đáp ứng động lực học của dầm sandwich composite cũng được nghiên cứu và thảo luận.

Từ khoá: dầm sandwich CNTRC kết tụ, khối lượng di động, lý thuyết biến dạng trượt bậc ba, phân tích động lực học

Viện Cơ học, Viện Hàn lâm khoa học và công nghệ Việt Nam, 18 Hoàng Quốc Việt, Hà Nội, Việt Nam

Liên hệ

Trần Thị Thơm, Viện Cơ học, Viện Hàn lâm khoa học và công nghệ Việt Nam, 18 Hoàng Quốc Việt, Hà Nội, Việt Nam

Email: ttthom@imech.vast.vn

Lịch sử

- Ngày nhận: 01-12-2022
- Ngày chấp nhận: 23-5-2023
- Ngày đăng: 30-6-2023

DOI :

https://doi.org/10.32508/stdjet.v6i1.1054

Trích dẫn bài báo này: Thơm T T, Hoài B T T, Kiên N D. **Ứng xử động lực học của dầm sandwich với các lớp ngoài gia cường bởi ống nano các-bon kết tụ chịu khối lượng di động sử dụng lý thuyết biến dạng trượt bậc ba**. *Sci. Tech. Dev. J. - Eng. Tech.* 2023; 6(1):1844-1854.